International Journal of Microwave and Wireless Technologies

cambridge.org/mrf

Plane and cylindrical waves scattering from a strip loaded single and double near zero metamaterial cylindrical object

Abdul Raqeeb, Zeeshan A. Awan and Arshad Hussain

Department of Electronics, Quaid-i-Azam University, Islamabad, 45320, Pakistan

Research Paper

Cite this article: Raqeeb A, Awan ZA, Hussain A (2025) Plane and cylindrical waves scattering from a strip loaded single and double near zero metamaterial cylindrical object. *International Journal of Microwave and Wireless Technologies* **17**(4), 567–581. https://doi.org/10.1017/S175907872500025X

Received: 31 May 2024
Revised: 7 February 2025
Accepted: 12 February 2025

Keywords:
metamaterials; scattering theory; scattering width; strip loaded cylindrical object

Corresponding author: Zeeshan A. Awan; Email: zeeshan@qau.edu.pk

Abstract

A rigorous analysis of the scattering of plane and cylindrical waves from a strip loaded single near zero and double near zero (DNZ) metamaterial cylindrical object is presented. The proposed problem has been solved using integral equations derived from Green's theorem and usual tangential boundary conditions. During the analysis, it was found that by loading a strip onto the metamaterial cylindrical objects, one can enhance or diminish the scattering under some specified conditions. It is shown that an enhancement in the back scattering occurs for a strip loaded DNZ metamaterial cylinder as compared to the back scattering of an unloaded DNZ metamaterial cylinder for both types of incident polarization. In the case of a specifically located electric line source, it is argued that by loading a strip onto a DNZ metamaterial cylinder, one can reduce the magnitude of the total field significantly at specific observation azimuth angles. For a specific location of a magnetic line source, the magnitude of total field of a strip loaded mu near zero (MNZ) metamaterial can be significantly enhanced as compared to unloaded MNZ cylinder in the specific observation directions. This parametric investigation is helpful in the designing of cylindrical metamaterial-based devices.

The scattering of plane and cylindrical waves by various dielectric cylindrical structures has been studied in many classical textbooks [1–3] and by authors [4–8] due to their important applications in microwave and optical regimes. Initially, the problem of electromagnetic scattering from a perfectly conducting strip loaded dielectric cylinder was studied by Elsherbeni and Hamid [9], which provides a useful model to study the scattering from the fuselage of an aircraft or rocket. They have solved the problem using integral equations derived from Green's theorem along with the applications of boundary conditions to transform the resulting integral equations into an equivalent matrix equation of infinite order. Asymptotic scattering of electromagnetic waves from an array of dielectrically loaded conducting strips under oblique incidence has been investigated by Elsherbeni and Jin [10]. They concluded that the scattering cross section of a perfectly conducting strip or an array of strips can be greatly minimized or maximized by loading each strip into a dielectric cylinder or dielectric shell. An analysis of the scattering properties of strip loaded circular dielectric cylinders has been carried out by Tsalamengas et al. [11] in the case of oblique incidence and arbitrary polarization. They found that the scattering characteristics can be controlled by varying the electromagnetic and geometrical parameters of the considered structure. Transverse magnetic (TM) and transverse electric (TE) scattering from strip loaded dielectric cylinders based on direct singular integral equation technique has been studied by Tsalamengas [12]. He has shown numerical results for dielectric cylinders loaded with flat or curved strips. An analytical solution of scattering from strip loaded lossy dielectric elliptic and circular cylinder has been investigated by Hamid and Hussein [13] using TM incident polarization. According to them, a significant reduction in echo width patterns can be found for different loss tangents using some specific parameters.

Recently, there has been a great deal of interest in the physics and engineering of single near zero (SNZ) and double near zero (DNZ) metamaterials due to their important technical applications [14–35]. An SNZ metamaterial can be further classified into epsilon near zero (ENZ) and mu near zero (MNZ) metamaterials. An ENZ metamaterial has its permittivity close to zero whereas an MNZ metamaterial has its permeability close to zero. A metamaterial having both permittivity and permeability close to zeros is called a double, near zero or near zero refractive index metamaterial. A DNZ metamaterial supports propagating modes with extremely large wavelength because its refractive index is very small, i.e., close to zero. These metamaterials with almost zero electromagnetic parameters can be used to realize energy tunneling [16–18], wavefront shaping [19, 20], directional emission [23, 24], and cloaking [27].

In this paper, scattering of plane and cylindrical waves from a strip loaded metamaterial cylinder is considered. The types of metamaterial considered in the present study are SNZ and

© The Author(s), 2025. Published by Cambridge University Press in association with The European Microwave Association.

DNZ. We have extended the work of Elsherbeni and Hamid [9] which was mainly relevant to the TM excitation of a strip loaded dielectric cylinder to the TE excitation, electric line source (ELS) and magnetic line source (MLS) excitations of a strip loaded metamaterial cylinder. We have also shown and discussed numerical results for each type of excitation whereas in [9], numerical results for only TM polarization have been shown and discussed. In the case of plane wave excitation, the obtained numerical results are also compared with CST simulations and a good agreement is found between them. During the study, it was found that a strip loaded DNZ metamaterial cylinder enhances the back scattering as compared to the back scattering of an unloaded DNZ metamaterial cylinder for both types of incident polarization. It is also noticed that a specifically located ELS can be used to significantly reduce the magnitude of total field from a strip loaded DNZ metamaterial cylindrical object at specific observation angles as compared to an unloaded DNZ metamaterial cylindrical object. Likewise, for a specifically located MLS excitation, the magnitude of total field of a strip loaded MNZ metamaterial can be significantly enhanced as compared to unloaded MNZ cylinder in the specific observation directions. These abovementioned findings are novel and have not been reported previously in the literature. This study is helpful in the design of cylindrical metamaterial based devices.

Formulation of the problem

To formulate the problem, an infinite length circular cylinder of fixed radius a is considered. The axial direction of a cylinder is parallel to the z-axis and the center of the cylinder coincides with the origin of the standard Cartesian coordinate system. This cylinder has electromagnetic parameters of $\varepsilon_1 = \varepsilon_o\varepsilon_{r1}$ and $\mu_1 = \mu_o\mu_{r1}$ where ε_o and μ_o are the permittivity and permeability of the free space, respectively. The parameters ε_{r1} and μ_{r1} represent the relative permittivity and relative permeability of the cylinder material, respectively. The material of the cylinder is taken to be linear, homogeneous, and isotropic. For the present theory, it is assumed that the material of a cylinder is lossless, but the proposed theory can also be used for lossy materials as well. A perfectly conducting strip of length $2a$ is located inside the cylinder which lies in the xz-plane and divides the cylinder into two regions, i.e., region 1 and region 2. This strip loaded cylinder is embedded in the free space background which occupies region 3. The geometrical configuration of strip loaded cylinders with plane wave and cylindrical wave excitation has been shown in Fig. 1(a) and (b), respectively. A time dependence of $e^{j\omega t}$ has been assumed and suppressed throughout.

Suppose there exists an electric field vector $\mathbf{E}$ and a magnetic field vector $\mathbf{H}$ due to a pair of sources, i.e., electric current density $\mathbf{J}$ and magnetic current density $\mathbf{M}$ outside the cylinder in region 3. Inside the cylinder, there exists an electric field vector $\mathbf{E}_m$ and a magnetic field vector $\mathbf{H}_m$ in the mth region with $m = 1, 2$. These electric and magnetic field vectors, i.e., $\mathbf{E}$, $\mathbf{H}$, $\mathbf{E}_m$, and $\mathbf{H}_m$ may exist within a surface S, enclosing a volume V, of a linear, homogeneous and isotropic medium. By using Green's vector theorem [36], we can write,

$$\int_s (\mathbf{E}_m \times \mathbf{H} - \mathbf{E} \times \mathbf{H}_m) \cdot \hat{\mathbf{n}} ds = \int_V (\mathbf{H}_m \cdot \mathbf{M} - \mathbf{E}_m \cdot \mathbf{J}) dV \quad (1)$$

where $\int_s$ and $\int_V$ represent the surface integral and the volume integral, respectively. Here $\hat{\mathbf{n}}$ is a unit vector normal to the cylinder at $\rho = a$, i.e., $\hat{\mathbf{n}} = \hat{\boldsymbol{\rho}}$.

Plane wave excitation

In the case of plane wave excitation, the strip loaded dielectric cylinder is illuminated by an incident plane wave. In order to analyze the complete scattering characteristics of this strip loaded material cylinder, both types of incident wave polarizations have been considered, i.e., TM and TE. The incident plane wave makes an angle ϕ_o with $+x$-axis as shown in Fig. 1(a). Here, the z-direction is taken to be the axial direction of a strip loaded cylinder. For TM polarization, the incident electric field is parallel to the z-axis, i.e., the incident electric field vector has only a nonzero z-component. On the other hand, for TE polarization, its incident magnetic field is parallel to the z-axis, which shows that the incident magnetic field vector has only a nonzero z-component.

For TM polarization, using the procedure as outlined in [9], the z-component of electric fields in all the three regions can be written in terms of cylindrical coordinates (ρ, ϕ, z) as below,

$$E_{3z} = E_o H_p^{(2)}(k_o\rho) e^{jp\phi}, \quad p = 0, \pm 1, \pm 2, \ldots \quad (2)$$

$$E_{1z} = E_o \sum_{n=1}^{\infty} C(n,p)\, J_n(k_1\rho) \sin(n\phi) \quad (3)$$

$$E_{2z} = E_o \sum_{m=1}^{\infty} D(m,p) J_m(k_1\rho) \sin(m(\phi - \pi)) \quad (4)$$

where $k_o = \omega\sqrt{\varepsilon_o\mu_o}$, $k_1 = \omega\sqrt{\varepsilon_1\mu_1}$ and E_o is the amplitude of the incident plane wave. Also, E_{uz} is the z-component of the electric field in uth region with $u = 1, 2, 3$ as shown in Fig. 1(a). Here $C(n,p)$ and $D(m,p)$ are unknown expansion coefficients which are needed to be determined. The function $J_n(\cdot)$ represents an nth order Bessel function of first kind and $H_p^{(2)}(\cdot)$ represents a pth order Hankel function of second kind. It should be noted that $H_p^{(2)}(k_o\rho)$ represents an outward traveling cylindrical wave for the assumed time convention. It can be shown that the electric field E_{3z} as given by Eq. (2) satisfies the radiation condition. In order to determine the unknown coefficients C and D, one may use the following boundary conditions,

$$E_{1z} = E_{3z}, \quad \rho = a, \quad 0 \le \phi \le \pi \quad (5)$$

$$E_{2z} = E_{3z}, \quad \rho = a, \quad \pi \le \phi \le 2\pi. \quad (6)$$

Using Eqs. (2)–(4) in the boundary conditions given by Eqs. (5) and (6) and after some manipulations, the unknown coefficients $C(n,p)$ and $D(m,p)$ can be found. Once these coefficients are known, we can find the z-components of the electric field in regions 1 and 2 as given by Eqs. (3) and (4). Likewise, the ϕ-components of the magnetic field in all three regions, i.e., $H_{u\phi}$ with $u = 1, 2, 3$, can be found from Maxwell's equations by taking $E_{u\rho} = E_{u\phi} = 0$. By following the steps as given in [9] and using Eq. (1) for all the three regions, we can write an equation in terms of the unknown electric field E_z at the boundary $\rho = a$ as below,

$$\int_0^{\pi} E_z H_{1\phi}\, d\phi + \int_{\pi}^{2\pi} E_z H_{2\phi}\, d\phi - \int_0^{2\pi} E_z H_{3\phi}\, d\phi = -\frac{4je^{j[p(\phi_o + \frac{\pi}{2}) + \frac{\pi}{2}]}}{\eta_o k_o a} E_o^2. \quad (7)$$

By substituting the ϕ-components of the magnetic fields of all the three regions, i.e., $H_{1\phi}$, $H_{2\phi}$, and $H_{3\phi}$ in above Eq. (7), we can write

https://doi.org/10.1017/S175907872500025X Published online by Cambridge University Press

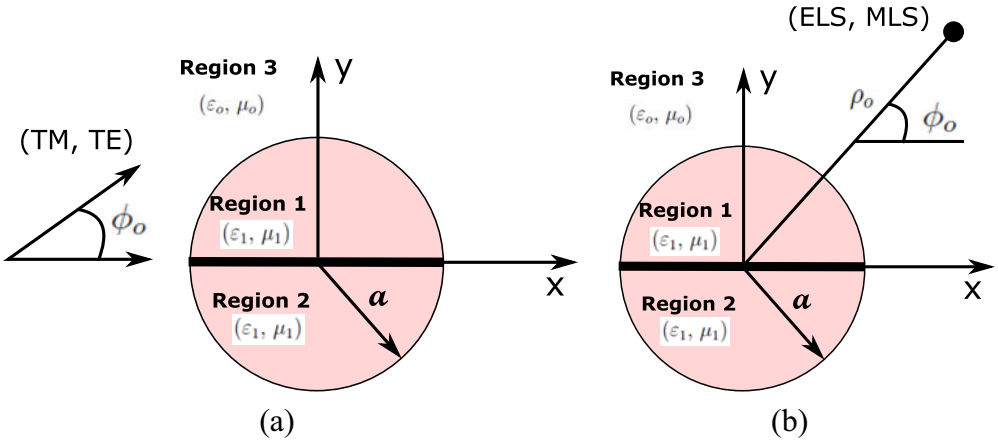


Figure 1. The geometrical configuration of strip loaded cylinders with (a) TM and TE plane wave excitation and (b) electric and magnetic line source excitation.

an equation in terms of the electric field E_z at the boundary $\rho = a$ which is given below,

$$\frac{1}{j\eta_1}\sum_{n=1}^{\infty} C(n,p)J_n'(k_1a)\int_0^{\pi} E_z \sin(n\phi)d\phi + \frac{1}{j\eta_1}\sum_{n=1}^{\infty} D(m,p)J_m'(k_1a)\int_{\pi}^{2\pi} E_z \sin(m(\phi-\pi))d\phi - \frac{1}{j\eta_o}H_p^{(2)\prime}(k_oa)\int_0^{2\pi} E_z e^{jp\phi}d\phi = -\frac{4je^{j[p(\phi_o+\frac{\pi}{2})+\frac{\pi}{2}]}}{\eta_o k_o a}E_o \quad (8)$$

where $(')$ denotes the differentiation with respect to the argument. Also, η_o is the intrinsic impedance of the free space and $\eta_1 = \sqrt{\mu_1/\varepsilon_1}$ is the intrinsic impedance of the material cylinder. The solution of the above Eq. (8) gives the values of the field E_z at the boundary $\rho =$ a. This electric field, E_z in region 3, can be expressed in the following series as,

$$E_z = E_o\sum_{q=-\infty}^{\infty} c_q^{TM}H_q^{(2)}(k_o\rho)e^{-jq\phi} \quad (9)$$

where c_q^{TM} is the unknown coefficient and needs to be determined. By substituting Eq. (9) in Eq. (8), the infinite set of equations in unknown c_q^{TM} can be found. In order to obtain the convergent results for coefficients c_q^{TM}, it is required to define the same truncation index N for both indices p and q which should be chosen large enough to give the accuracy required. Thus, the final equation for unknown c_q^{TM} is given below,

$$\frac{1}{\eta_1}\sum_{q=-N,q\neq p}^{N} c_q^{TM}H_q^{(2)}(k_oa)f_c(p,q) + \frac{1}{\eta_1}c_p^{TM}H_p^{(2)}(k_oa)\cdot f_c(p,p) - \frac{2\pi}{\eta_o}c_p^{TM}H_p^{(2)\prime}(k_oa)H_p^{(2)}(k_oa) = \frac{4e^{j[p(\phi_o+\frac{\pi}{2})+\frac{\pi}{2}]}}{\eta_o k_o a} \quad (10)$$

$$f_c(p,q) = \sum_{n=1}^{\infty} C(n,p)J_n'(k_1a)f_a(n,q) + \sum_{m=1}^{\infty} D(m,p)\cdot J_m'(k_1a)f_b(m,q) \quad (11)$$

where $f_a(n,q)$ and $f_b(m,q)$ have been defined by Eqs. (19) and (20) in [9]. The coefficient c_q^{TM} is determined numerically by solving Eqs. (10) and (11). In region 3, the z-component of the total electric field E_z^t can be taken as a sum the incident plane wave and the z-component of the scattered electric field from the strip loaded material cylinder. For this, it is desired to express the incident plane wave as an infinite sum of cylindrical waves [2]. Likewise, the z-component of the scattered field can also be expressed in terms of an infinite sum of outward traveling cylindrical waves with the unknown scattering amplitude coefficient D_n^{TM}. Mathematically, the total electric field E_z^t can be expressed as below,

$$E_z^t = E_o\sum_{n=-\infty}^{\infty}[j^nJ_n(k_o\rho) + D_n^{TM}H_n^{(2)}(k_o\rho)]e^{-jn(\phi-\phi_o)} \quad (12)$$

where D_n^{TM} is the unknown and can be found by comparing Eqs. (9) and (12) at $\rho = a$ as below,

$$D_n^{TM} = c_n^{TM}e^{-jn\phi_o} - \frac{j^nJ_n(k_oa)}{H_n^{(2)}(k_oa)}. \quad (13)$$

Here D_n^{TM} is known provided that if c_n^{TM} is known. In the case of a perfectly electric conducting (PEC) cylinder without a strip, it can be shown that $c_n^{TM} = 0$ and D_n^{TM} becomes as,

$$D_n^{TM} = -\frac{j^nJ_n(k_oa)}{H_n^{(2)}(k_oa)}. \quad (14)$$

In the case of a material cylinder without a strip, the coefficient D_n^{TM} can be found by applying the usual tangential boundary conditions at $\rho = a$ for $0 \le \phi \le 2\pi$. Thus, using this information and following the procedure as outlined above, the coefficient D_n^{TM} for a material cylinder without a strip becomes as,

$$D_n^{TM} = -j^n\frac{\eta_1J_n'(k_oa)J_n(k_1a) - \eta_oJ_n(k_oa)J_n'(k_1a)}{\eta_1H_n^{(2)\prime}(k_oa)J_n(k_1a) - \eta_oH_n^{(2)}(k_oa)J_n'(k_1a)}. \quad (15)$$

For TE polarization, we do not have a component of the electric field in the z-direction for all the considered three regions, i.e., $E_{uz} = 0$ and $H_{uz} \neq 0$ with $u = 1, 2, 3$. Extending the same procedure as outlined above for the TE case, the z-components of magnetic fields in all three regions can be written in terms of cylindrical coordinates as below,

$$H_{3z} = \frac{E_o}{j\eta_o}H_p^{(2)}(k_o\rho)e^{jp\phi}, \quad p = 0, \pm1, \pm2, \ldots \quad (16)$$

$$H_{1z} = \frac{E_o}{j\eta_1}\sum_{n=1}^{\infty}A(n,p)J_n(k_1\rho)\sin(n\phi) \quad (17)$$

$$H_{2z} = \frac{E_o}{j\eta_1}\sum_{m=1}^{\infty}B(m,p)J_m(k_1\rho)\sin(m(\phi-\pi)) \quad (18)$$

https://doi.org/10.1017/S175907872500025X Published online by Cambridge University Press

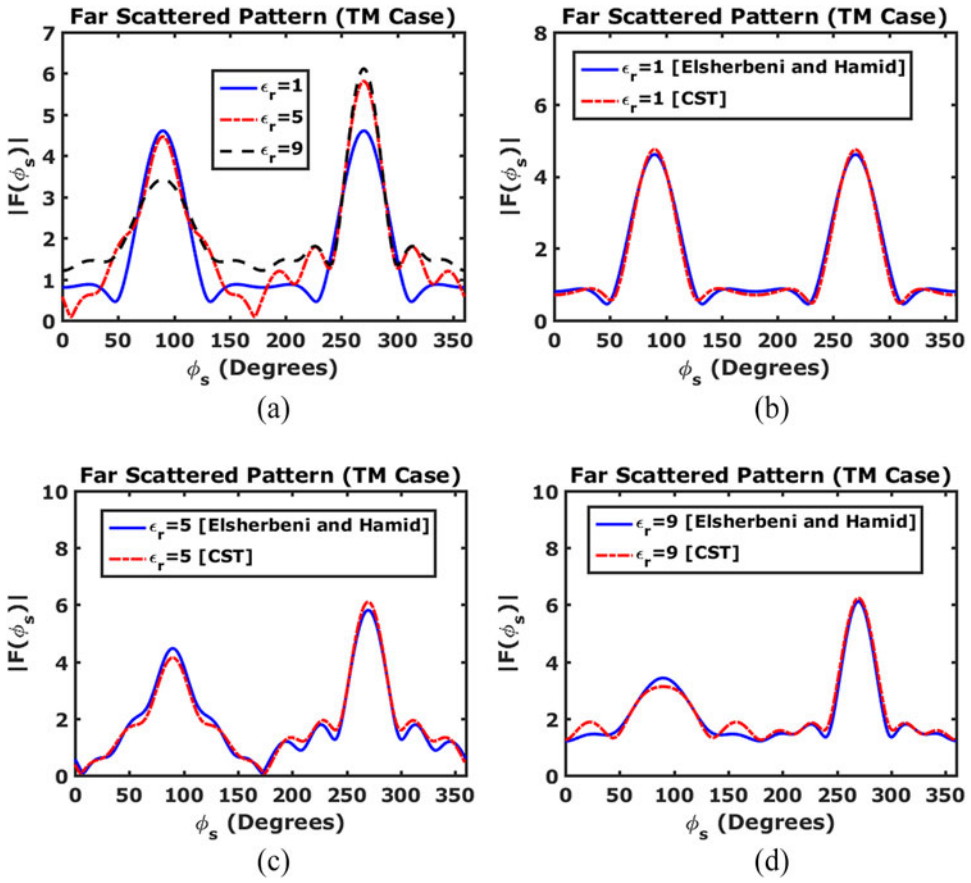


Figure 2. (a) Reproduced far scattered field patterns of strip loaded dielectric cylinder due to a TM incident plane wave based on the proposed theory as given in Figure 5(b) of Elsherbeni and Hamid [9]. Here $\phi_o = 90^\circ$, $ka = 5$, and $\epsilon_r = 1, 5$, and 9, which are adopted from [9]. (b)–(d) Far scattered field patterns as given in part (a) and their comparisons with the CST simulations.

where $A(n,p)$ and $B(m,p)$ are the unknown expansion coefficients and can be determined using the following boundary conditions as given below,

$$H_{1z} = H_{3z}, \quad \rho = a, \quad 0 \le \phi \le \pi \tag{19}$$

$$H_{2z} = H_{3z}, \quad \rho = a, \quad \pi \le \phi \le 2\pi. \tag{20}$$

Once the coefficients $A(n,p)$ and $B(m,p)$ become known, then the z-components of magnetic fields in regions 1 and 2 can be determined by Eqs. (17) and (18). The ϕ-components of the electric fields in all three regions, i.e., $E_{1\phi}$, $E_{2\phi}$, and $E_{3\phi}$, can be found from Maxwell's equations. Using Eq. (1) for all three regions, we can develop an equation similar to Eq. (7) for the considered TE polarization in terms of an unknown electric field E_ϕ at $\rho = a$ and z-components of the magnetic fields in all three regions, i.e., H_{1z}, H_{2z}, and H_{3z}. For the unknown electric field E_ϕ in region 3, the following series expansion can be used, i.e.,

$$E_\phi = E_o \sum_{q=-\infty}^{\infty} C_q^{TE} H_q^{(2)\prime}(k_o\rho) e^{-jq\phi} \tag{21}$$

where C_q^{TE} is the unknown. Following the same steps as adopted for TM case, we can write an equation in unknown C_q^{TE} as below,

$$\sum_{q=-N, q\neq p}^{N} C_q^{TE} H_q^{(2)}(k_o a) f_c(p,q) + C_p^{TE} H_p^{(2)}(k_o a) f_c(p,p) - 2\pi C_p^{TE} H_p^{(2)\prime}(k_o a) H_p^{(2)}(k_o a) = -\frac{4e^{j[p(\phi_o+\frac{\pi}{2})+\frac{\pi}{2}]}}{k_o a}. \tag{22}$$

The unknown C_q^{TE} can be made known by solving Eq. (22) numerically and adopting similar conditions as used for the TM case. The ϕ-component of total electric field in region 3 can also be expressed in terms of the unknown scattering coefficient d_n^{TE} as below,

$$E_\phi^t = E_o \sum_{n=-\infty}^{\infty} [j^n J_n'(k_o\rho) + d_n^{TE} H_n^{(2)\prime}(k_o\rho)] e^{-jn(\phi-\phi_o)}. \tag{23}$$

By comparing Eqs. (21) and (23) at $\rho = a$, the unknown scattering coefficient d_n^{TE} can be found and given below,

$$d_n^{TE} = C_n^{TE} e^{-jn\phi_o} - \frac{j^n J_n'(k_o a)}{H_n^{(2)\prime}(k_o a)}. \tag{24}$$

Here d_n^{TE} is known provided that if C_n^{TE} is known. In the case of a PEC cylinder, we have $C_n^{TE} = 0$ and d_n^{TE} becomes as,

$$d_n^{TE} = -\frac{j^n J_n'(k_o a)}{H_n^{(2)\prime}(k_o a)}. \tag{25}$$

https://doi.org/10.1017/S175907872500025X Published online by Cambridge University Press

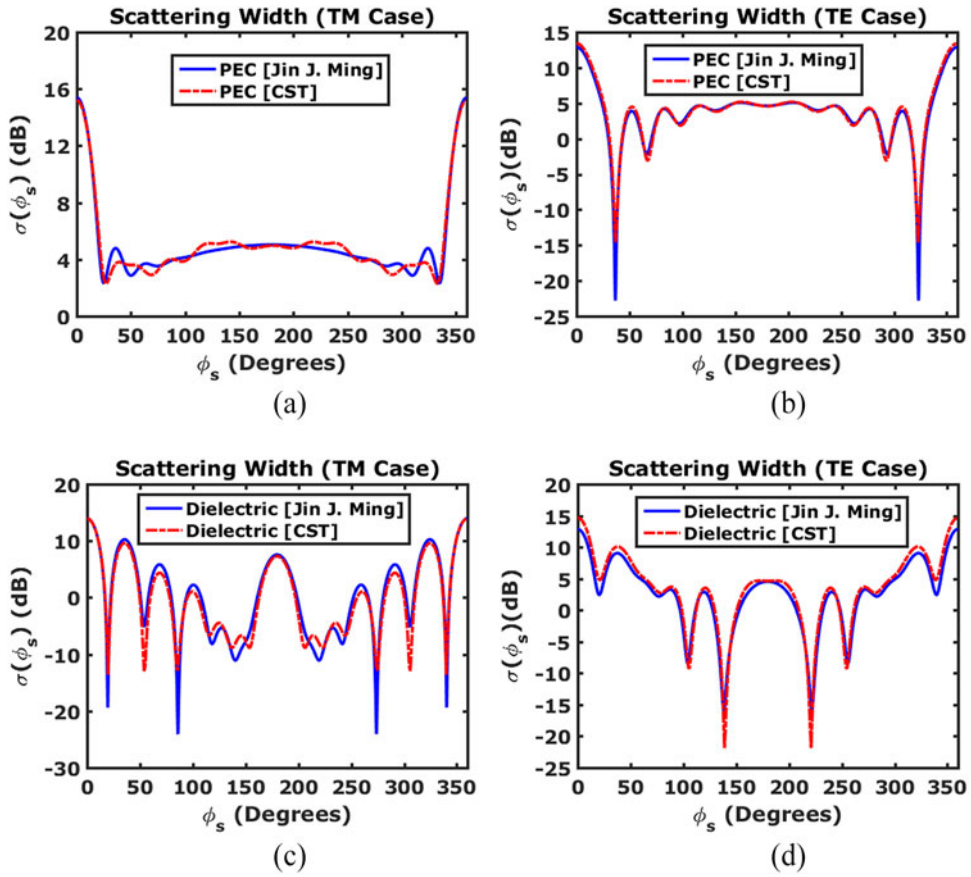


Figure 3. The normalized scattering widths of a perfectly electric conducting (PEC) cylindrical object for (a) TM and (b) TE cases are based on proposed theory and their comparisons with respective scattering widths computed using CST studio. The normalized scattering widths of a dielectric cylindrical object for (c) TM and (d) TE polarizations are based on proposed theory and their comparisons with respective scattering widths simulated using CST studio. For both PEC and dielectric cylindrical objects, electromagnetic and geometrical parameters have been adopted from Jin [3].

Following the same procedure as outlined above, the coefficient d_n^{TE} for a dielectric cylinder without a strip becomes as,

$$d_n^{TE} = -j^n \frac{\eta_o J_n'(k_o a) J_n(k_1 a) - \eta_1 J_n(k_o a) J_n'(k_1 a)}{\eta_o H_n^{(2)\prime}(k_o a) J_n(k_1 a) - \eta_1 H_n^{(2)}(k_o a) J_n'(k_1 a)}. \quad (26)$$

In the present study, the scattering width is a quantity of interest for both types of incident polarization. For this, it is required to find the far zone scattered field pattern, i.e., $F_{TM}(\phi)$ and $F_{TE}(\phi)$ which can be found from the second term of Eqs. (12) and (23) after using the large argument approximation of the Hankel function and its derivative, respectively. They are given below,

$$F_{TM}(\phi) = \sum_{n=-\infty}^{\infty} D_n^{TM} j^n e^{-jn(\phi-\phi_o)} \quad (27)$$

$$F_{TE}(\phi) = -\sum_{n=-\infty}^{\infty} d_n^{TE} j^{n+1} e^{-jn(\phi-\phi_o)}. \quad (28)$$

Based upon these above far zone scattered field patterns, the normalized scattering width [2], i.e., $\sigma(\phi) = \sigma_{2D}(\phi)/\lambda_o$, can be written as below with $p = TM, TE$,

$$\sigma(\phi) = \frac{2}{\pi}|F_p(\phi)|^2 \quad (29)$$

where λ_o is the wavelength in the background free space medium.

Line source excitation

In the previous section, the source of excitation is taken to be the plane wave, which is independent of the location of source. Contrary to this, if a strip loaded material cylinder is excited by a line source, then the location of source plays an important role for modeling the complete scattering characteristics. For this case, two types of line sources can be considered. (1) An ELS with the magnitude of electric current I and (2) MLS with the magnitude of magnetic current I_m. It is assumed that the locations of both line sources are assumed to be (ρ_o, ϕ_o) in the usual cylindrical coordinates and their axial directions are taken to be parallel to the axial direction of strip loaded material cylinder, i.e., z-axis. This geometrical configuration has been shown in Fig. 1(b).

In the first case, an ELS excitation has been assumed. For this case, the total electric field, E_z^l which is the sum of incident and scattered electric fields, can be written as below [2],

$$E_z^l = \begin{cases} \frac{-\eta_o k_o}{4} \sum_{n=-\infty}^{\infty} [IJ_n(k_o\rho) + E_n H_n^{(2)}(k_o\rho)] \\ \cdot H_n^{(2)}(k_o\rho_o) e^{-jn(\phi-\phi_o)}, \quad a \le \rho < \rho_o \\ \\ \frac{-\eta_o k_o}{4} \sum_{n=-\infty}^{\infty} [IJ_n(k_o\rho_o) + E_n H_n^{(2)}(k_o\rho_o)] \\ \cdot H_n^{(2)}(k_o\rho) e^{-jn(\phi-\phi_o)}, \quad \rho > \rho_o \end{cases} \quad (30)$$

https://doi.org/10.1017/S175907872500025X Published online by Cambridge University Press

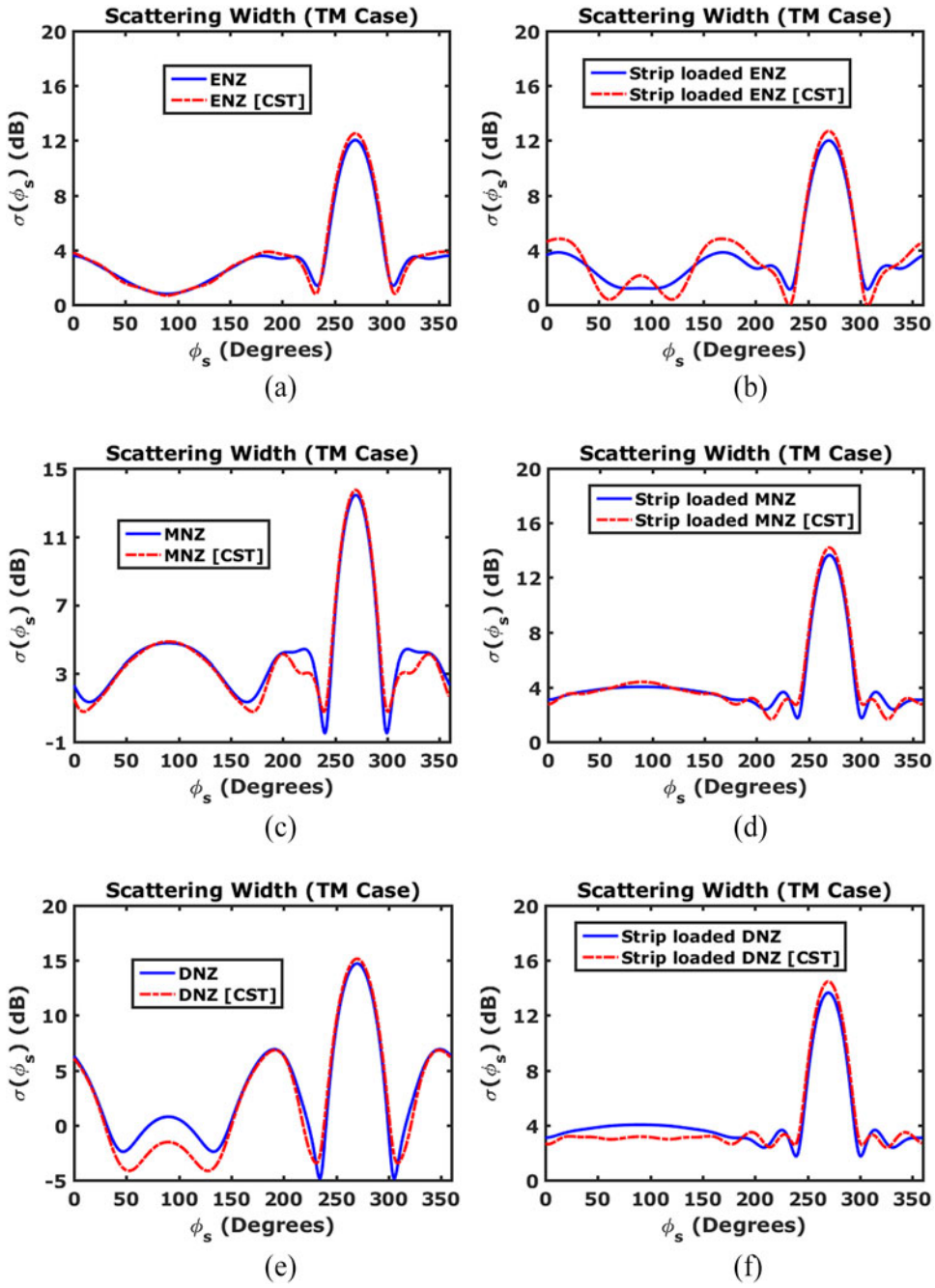


Figure 4. The normalized scattering widths of (a) ENZ, (b) strip loaded ENZ, (c) MNZ, (d) strip loaded MNZ, (e) DNZ, and (f) strip loaded DNZ cylinders and their comparisons with the normalized scattering widths computed using CST studio for TM polarization.

where E_n is the unknown scattering coefficient and can be found by comparing the total electric field in region 3 as given by Eq. (9) to the total electric field as given by Eq. (30) at $\rho = a$. Using this above procedure, it is found that the unknown scattering coefficient E_n can be written as,

$$E_n = -\frac{4E_o c_n^{TM} e^{-jn(\phi_o)}}{\eta_o k_o H_n^{(2)}(k_o \rho_o)} - \frac{IJ_n(k_o a)}{H_n^{(2)}(k_o a)}. \tag{31}$$

In the case of a material cylinder without a strip, the unknown scattering coefficient E_n can be written in terms of coefficient D_n^{TM} as below,

$$E_n = \frac{D_n^{TM} I}{j^n} \tag{32}$$

where D_n^{TM} has been derived previously and given by Eq. (15).

https://doi.org/10.1017/S175907872500025X Published online by Cambridge University Press

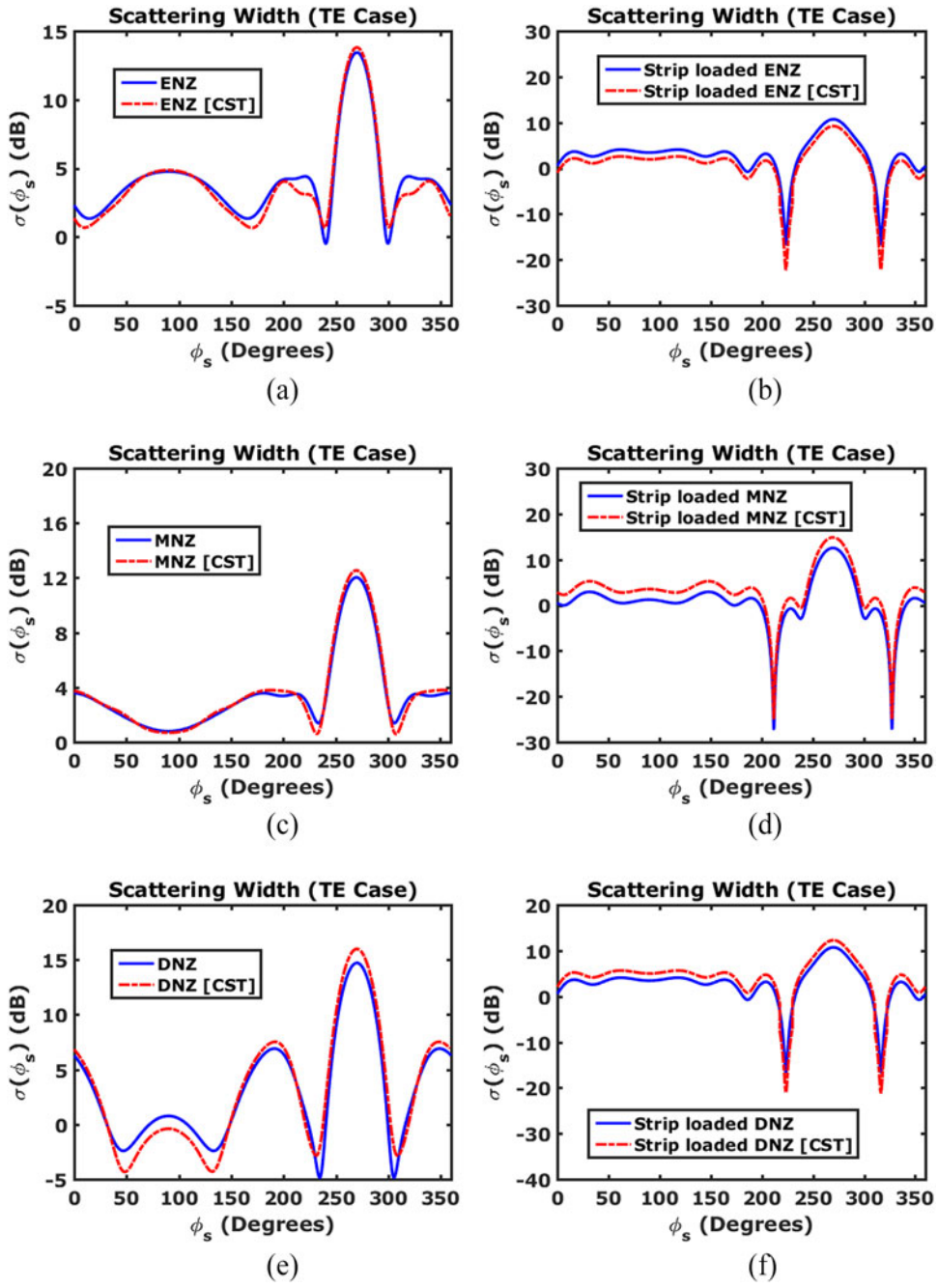


Figure 5. The normalized scattering widths of (a) ENZ, (b) strip loaded ENZ, (c) MNZ, (d) strip loaded MNZ, (e) DNZ, and (f) strip loaded DNZ cylinders and their comparisons with the normalized scattering widths computed using CST studio for TE polarization.

In the case of a strip loaded material cylinder when excited by an MLS, the total magnetic field H_z^m is a sum of the incident magnetic field and the scattered magnetic field, which is given below,

$$H_z^m = \begin{cases} \frac{-k_o}{4\eta_o} \sum_{n=-\infty}^{\infty} [I_m J_n(k_o\rho) + M_n H_n^{(2)}(k_o\rho)] \\ \cdot H_n^{(2)}(k_o\rho_o) e^{-jn(\phi-\phi_o)}, \quad a \le \rho < \rho_o \\ \\ \frac{-k_o}{4\eta_o} \sum_{n=-\infty}^{\infty} [I_m J_n(k_o\rho_o) + M_n H_n^{(2)}(k_o\rho_o)] \\ \cdot H_n^{(2)}(k_o\rho) e^{-jn(\phi-\phi_o)}, \quad \rho > \rho_o \end{cases} \tag{33}$$

where M_n is the unknown scattering coefficient and needs to be determined. Using Maxwell's equation, we can find E_ϕ^m. Now, by comparing E_ϕ^m with the total electric field E_ϕ in region 3, which is given by Eq. (21) at $\rho = a$, we can find the coefficient M_n as below,

$$M_n = -\frac{4E_o C_n^{TE} e^{-jn\phi_o}}{jk_o H_n^{(2)}(k_o\rho_o)} - \frac{I_m J_n'(k_o a)}{H_n^{(2)\prime}(k_o a)}. \tag{34}$$

For a material cylinder without a strip, the coefficient M_n becomes,

$$M_n = \frac{d_n^{TE} I_m}{j^n} \tag{35}$$

https://doi.org/10.1017/S175907872500025X Published online by Cambridge University Press

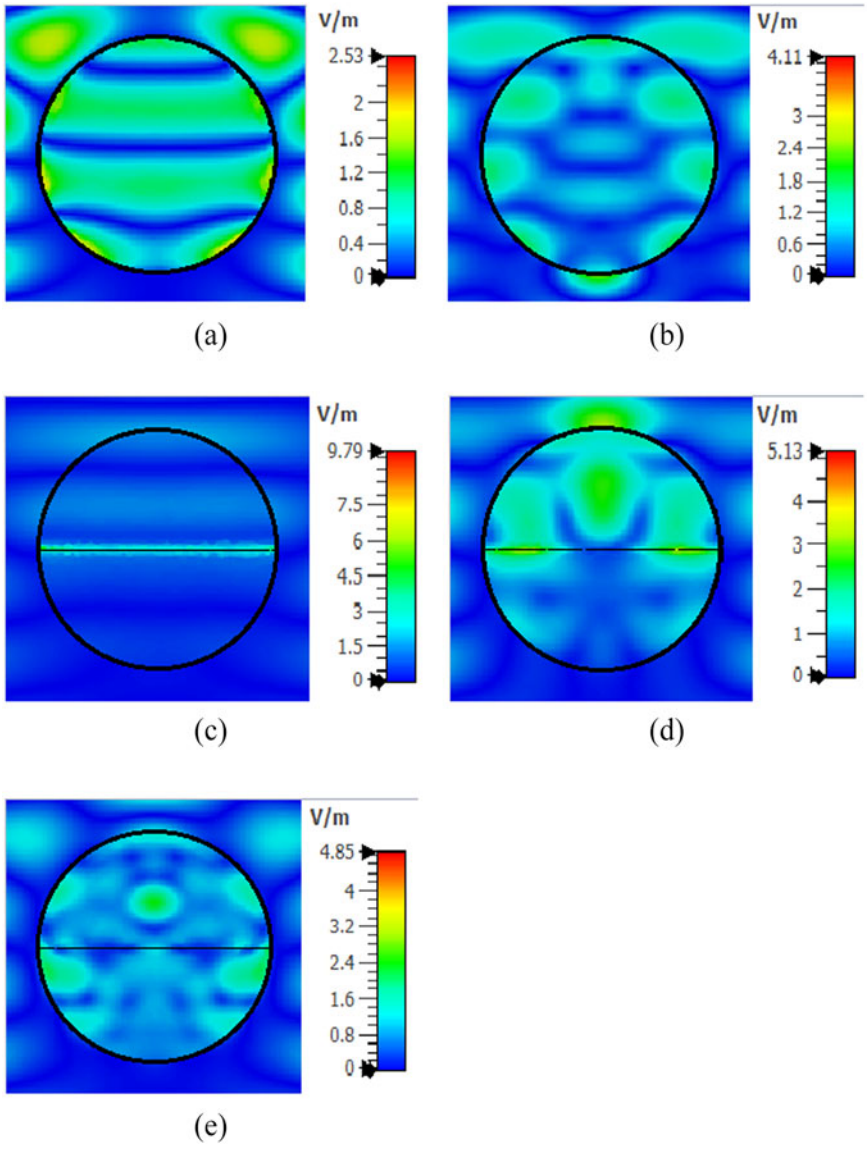


Figure 6. The electric field distribution for (a) PEC cylinder and (b) dielectric cylinder with $\epsilon_r = 4$ and strip loaded dielectric cylinders with (c) $\epsilon_r = 1$, (d) $\epsilon_r = 5$ and (e) $\epsilon_r = 9$. These electric field distributions have been computed using CST.

where the coefficient d_n^{TE} is given by Eq. (26). For both types of line source excitation, we are interested in the total field pattern, i.e., $F_l(\phi)$ with $l =$ ELS, MLS, and are given below,

$$F_{ELS}(\phi) = \frac{-\eta_o k_o}{4} \sum_{n=-\infty}^{\infty} j^n [IJ_n(k_o\rho_o) + E_n \cdot H_n^{(2)}(k_o\rho_o)] e^{-jn(\phi-\phi_o)} \quad (36)$$

$$F_{MLS}(\phi) = \frac{-k_o}{4\eta_o} \sum_{n=-\infty}^{\infty} j^n [I_m J_n(k_o\rho_o) + M_n \cdot H_n^{(2)}(k_o\rho_o)] e^{-jn(\phi-\phi_o)}. \quad (37)$$

Numerical results and discussions

In this section, numerical results have been shown and discussed along with the demonstration of the validation of the proposed formulation. For all numerical results, we have assumed $\phi_s = \phi$, $\epsilon_r = \varepsilon_{r1}$, and $\mu_r = \mu_{r1}$. Likewise, the size parameters of all strips loaded metamaterial cylindrical objects and metamaterial cylindrical objects without strips are assumed to be $ka = 5$ with $\phi_o = 90^\circ$ for all figures except Figs. 3 and 10 where they are different and mentioned accordingly. It should be noted that for $\phi_o = 90^\circ$, the forward scattering direction is characterized by an angle of $\phi_s = 270^\circ$ and the back scattering direction occurs for $\phi_s = 90^\circ$. In order to ensure the convergent results for the summations appearing in Eqs. (10) and (21), it is required to define the truncation index N. Here N is the absolute value of the upper limit of the index of summation in the series expressions. The typical value of the truncation index N is taken to be equal to k_1a+5 as given by [38, 39]. It should be noted that for all the numerical results related to "Numerical results and discussions" section, E_o is taken to be unity.

In order to validate the proposed formulation, the reproduced far scattered field patterns of a strip loaded dielectric cylinder or

https://doi.org/10.1017/S175907872500025X Published online by Cambridge University Press

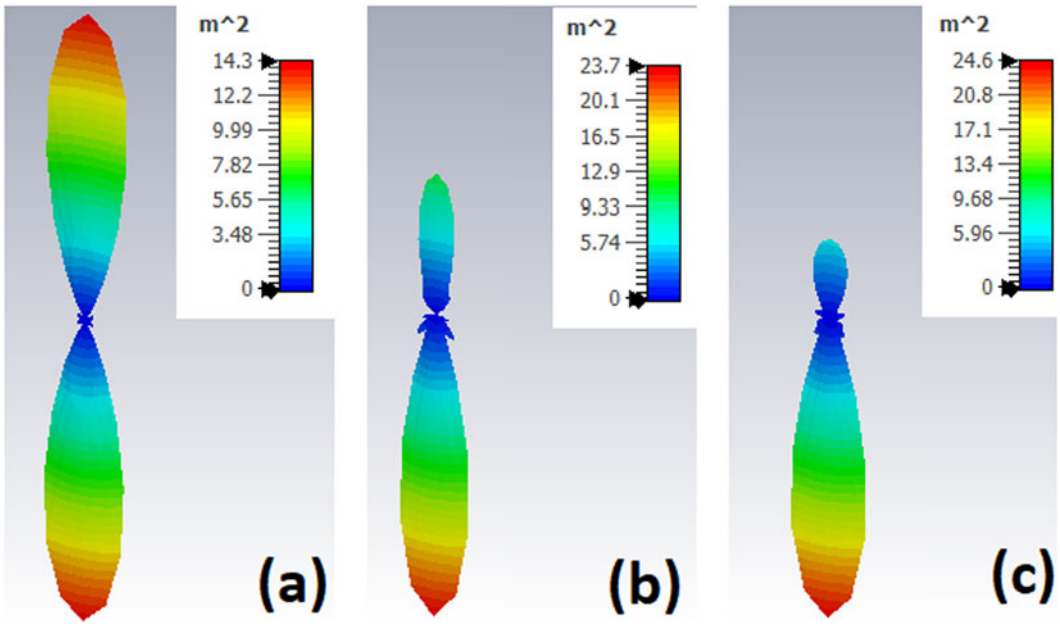


Figure 7. Three-dimensional scattering width patterns for strip loaded dielectric cylinders with (a) $\epsilon_r = 1$, (b) $\epsilon_r = 5$ and (c) $\epsilon_r = 9$ and have been computed using CST.

cylindrical object with variable values of ϵ_r have been shown in Fig. 2(a) which are in good agreement with those given in Fig. 5(b) of Elsherbeni and Hamid [9]. Likewise, these reproduced far scattered field patterns are compared with CST in Fig. 2(b)–(d). In Fig. 3, the normalized scattering widths of PEC and dielectric cylindrical objects without a strip based on the proposed theory have been shown and compared with their respective normalized scattering widths simulated using CST for both types of incident polarization, i.e., TM and TE. Here the radius of both cylinders are taken to be equal to free space wavelength. Also, $\epsilon_r = 4$ for a dielectric cylinder. The agreement between the proposed theory and simulated results obtained using CST is good. These findings validate the accuracy of the proposed formulation presented in this paper.

Figure 3 deals with the normalized scattering widths of PEC and dielectric cylinders, which are based on the proposed theory and their comparisons with the normalized scattering widths of respective cylinders using CST simulations. In this case, all electromagnetic and geometrical parameters have been taken from [3]. It is found that the normalized scattering widths of PEC and dielectric cylinders based on the proposed theory are in excellent agreement with Figs. 6.10(e)–(f) and 6.12(e)–(f) of Jin [3]. Some discrepancies in the scattering widths are apparent between the proposed theory and CST. This is because of the finite length cylinder assumption used in CST and the infinite length cylinder assumption which is adopted for proposed formulations. In Figs. 4–5, the normalized scattering widths of strip loaded ENZ, MNZ, and DNZ cylindrical objects along with their comparisons of respective normalized scattering widths for these metamaterial cylindrical objects without strip have been shown for both types of incident polarizations, i.e., TM and TE. These scattering widths are also compared with scattering widths simulated using CST. The electromagnetic parameters of ENZ, MNZ, and DNZ metamaterial cylinders have been taken from [37]. For ENZ cylinder, we have assumed $\epsilon_r = 10^{-3}$, $\mu_r = 1$ and for MNZ cylinder, it is assumed that $\epsilon_r = 1$, $\mu_r = 10^{-3}$. Likewise, for a DNZ cylinder, it is assumed that $\epsilon_r = 10^{-3}$ and $\mu_r = 10^{-3}$. It is clear from Fig. 4 that the forward scattering widths of strip loaded cylinders and strip unloaded cylinders have almost the same forward scattering widths for ENZ, MNZ, and DNZ metamaterials. It is seen that an enhancement of 3 dB occurs in the back scattering width as compared to the back scattering width of a DNZ cylinder without a strip in the case of TM polarization. It is argued from Fig. 5(e)–(f) that by loading a strip onto a DNZ cylinder, the forward SW diminishes by almost 4 dB and back SW enhances by 3 dB as compared to an unloaded DNZ cylinder.

The electric field distributions inside and outside of PEC, dielectric cylinder with $\epsilon_r = 4$, and strip loaded dielectric cylinders with $\epsilon_r = 1, 5, 9$ have been shown in Figs. 6(a)–(e). It is observed from Fig. 6(d)–(e) that with an increase in the value of ϵ_r from 4 to 9, the concentration of electric field below the strip increases. It is seen from Fig. 7 that for $\epsilon_r = 1$, the cylinder is absent, and the three-dimensional field pattern is the same as that of the three-dimensional field pattern of an isolated strip placed in the free space background. It is also observed that it has almost identical scattering in the forward and back scattering directions. As the value of ϵ_r increases from 5 to 9, then the forward scattering increases and backward scattering decreases. These findings can also be confirmed by Fig. 2(a). The electric field and magnetic field distributions inside and outside unloaded and strip loaded ENZ, MNZ, and DNZ cylindrical objects have been shown in Figs. 8 and 9, respectively.

It is well known that for plane wave excitation, the scattering characteristics of a scatterer, e.g., a cylindrical object, are independent of the location of the plane wave source. Contrary to this, if the same cylindrical object is excited by an ELS or MLS, then its scattering characteristics do depend upon location of line source excitation, i.e., ρ_o and ϕ_o and have been discussed and shown in Figs. 10–12. In order to validate the proposed theory of line source excitations, we have considered only ELS excitation, whereas similar findings can be found for MLS excitation. For an ELS excitation of a strip loaded dielectric cylinder based on the proposed theory, we have assumed that ϵ_r approaches to infinity with $\mu_r = 1$. In this case, it is found that coefficients c_n^{TM} become zero in

https://doi.org/10.1017/S175907872500025X Published online by Cambridge University Press

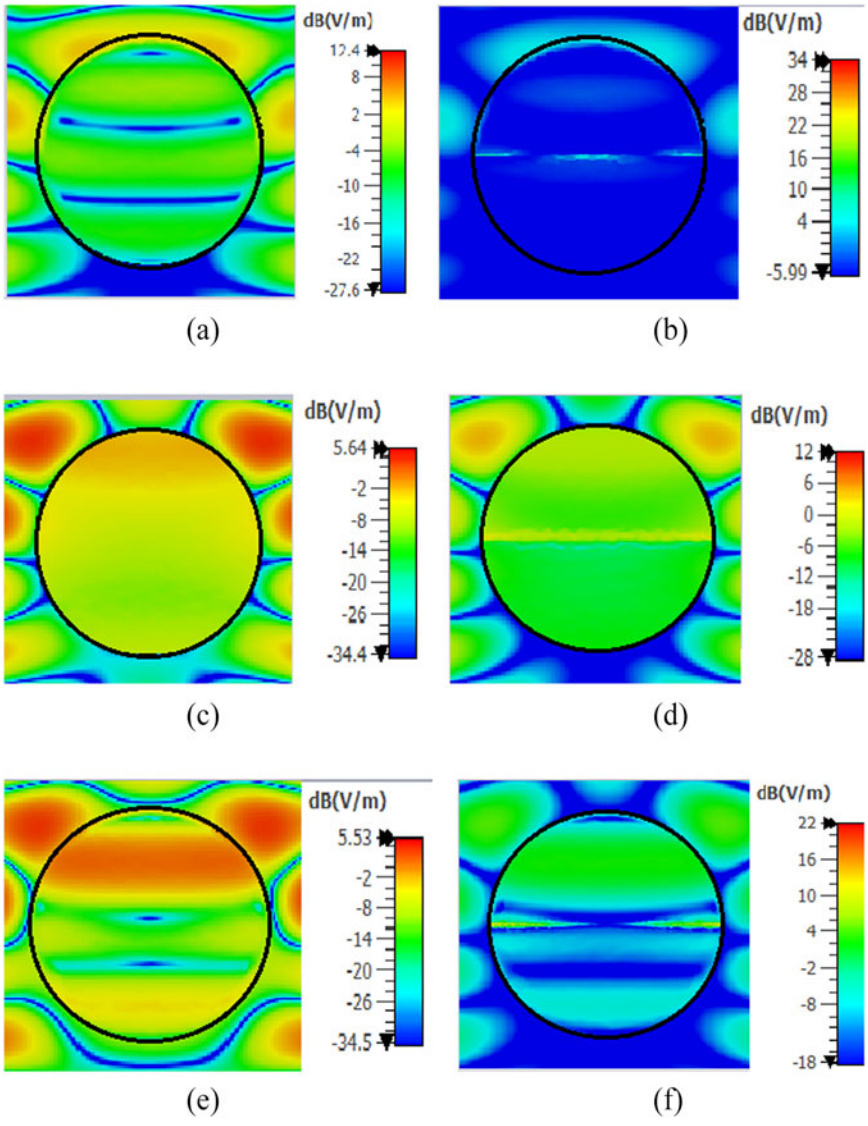


Figure 8. The electric field distribution for (a) ENZ cylinder, (b) strip loaded ENZ cylinder, (c) MNZ cylinder, (d) strip loaded MNZ cylinder, (e) DNZ cylinder, and (f) strip loaded DNZ cylinder due to TM polarization which has been computed using CST.

Eq. (31) and coefficients E_n reduce to the well-known scattering coefficients of a perfectly conducting cylinder [2]. Using these reduced coefficients E_n in Eq. (36), we can find that the total field pattern $F_{ELS}(\phi_s)$ becomes equivalent to the total field pattern of a PEC cylinder. This normalized total field pattern, i.e., $F_{ELS}(\phi_s)/F_1$ with $F_1 = (Ik_o\eta_o)/4$, has been shown in Fig. 10(a) based on the proposed theory for $k_o a = 10\pi$, $\phi_o = 0$, $\rho_o = 5.25\lambda_o$, and $\rho_o = 5.5\lambda_o$ at an operating free space wavelength λ_o of 0.1 m. These geometrical parameters have been adopted from Balanis [2]. It is found from Fig. 10(a) that the magnitudes of the normalized total field pattern are in good agreement with those reported by Balanis. In the second case, we have used our proposed theory of ELS excitation of a dielectric cylinder without strip and computed the scattering gain $G(\phi_s)$ based on the theory as given by Aslam et al. [40]. Also, we have assumed $\epsilon_r = 2, \mu_r = 1, k_o a = \pi$, $\phi_o = 0$, and $\rho_o = 0.9\lambda_o$ as adopted in [40]. It is clear from Fig. 10(b) that the proposed theory is in good agreement with those of Aslam et al. These agreements validate the proposed formulation presented in this paper for ELS excitation. The influence of ELS and MLS locations upon the magnitude of far zone total field patterns of strip loaded and unloaded metamaterial cylinders have been shown in Figs. 11–12. For these figures, it is assumed that $\phi_o = 0$. It is studied from Fig. 11(a) that the magnitude of total field of an unloaded ENZ cylinder becomes −35 dB at $\phi_s = 259°$, 281° with an ELS location of $\rho_o = 0.9\lambda_o$. If the same ENZ cylinder is loaded with a strip, then, the total field becomes −20 dB at angles $\phi_s = 259°$ and 281°. From here, it is concluded that an embedded strip can be used to enhance the total electric field of an ENZ cylinder by 15 dB at these specific angles. Likewise, for an ELS location of $\rho_o = 1.8\lambda_o$, the total field of an MNZ cylinder is −17 dB for angles $\phi_s = 265°$ and 275° which is shown in Fig. 11(d). In this case, the total field of a strip loaded MNZ cylinder becomes −32 dB at these specific angles of ϕ_s. This shows a reduction of the total field by 15 dB due to strip loading. It is observed from Fig. 11(f) that for $\rho_o = 1.8\lambda_o$, the total field of an unloaded DNZ cylinder is −12 dB at angles of $\phi_s = 262°$ and 274°. For this specific case, the total field becomes −32 dB for a strip loaded DNZ cylinder at $\phi_s = 262°, 274°$. Thus, it is argued that by loading a strip,

https://doi.org/10.1017/S175907872500025X Published online by Cambridge University Press

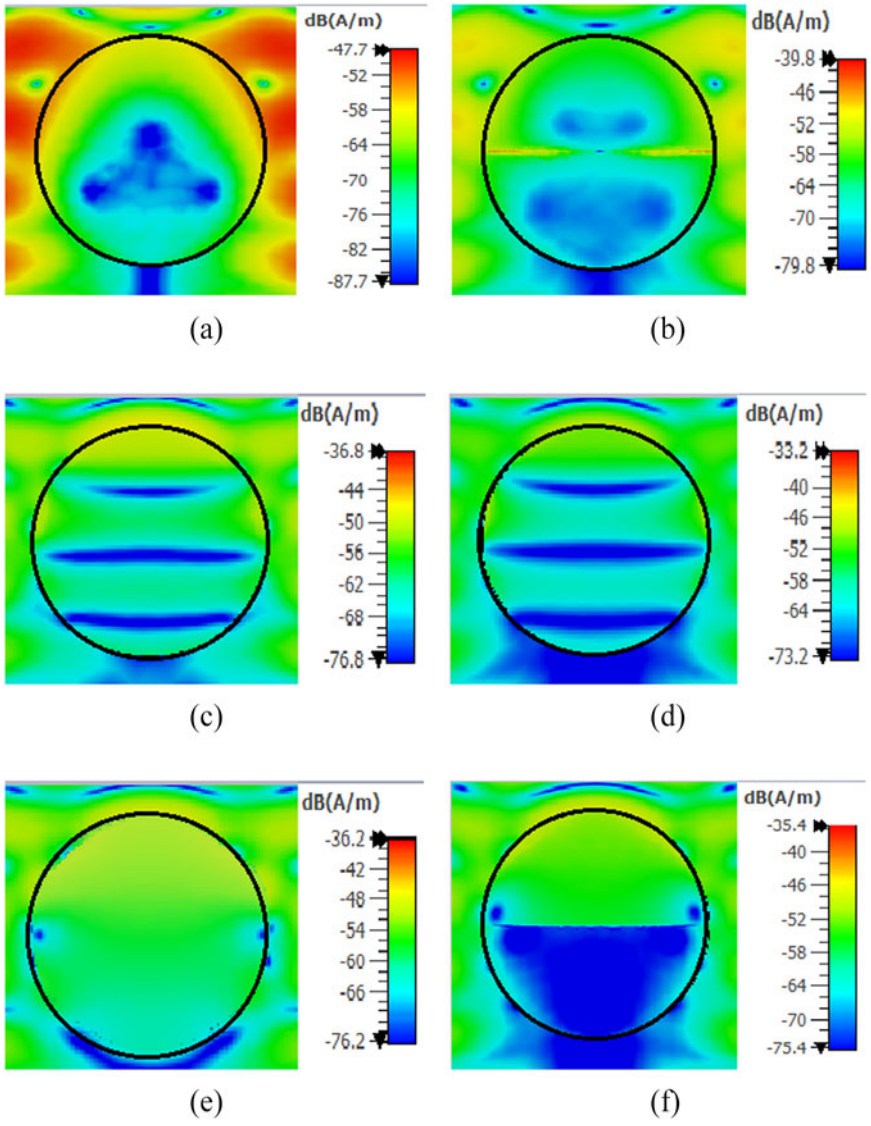


Figure 9. The magnetic field distribution computed using CST for (a) ENZ cylinder, (b) strip loaded ENZ cylinder, (c) MNZ cylinder, (d) strip loaded MNZ cylinder, (e) DNZ cylinder, and (f) strip loaded DNZ cylinder due to TE polarization.

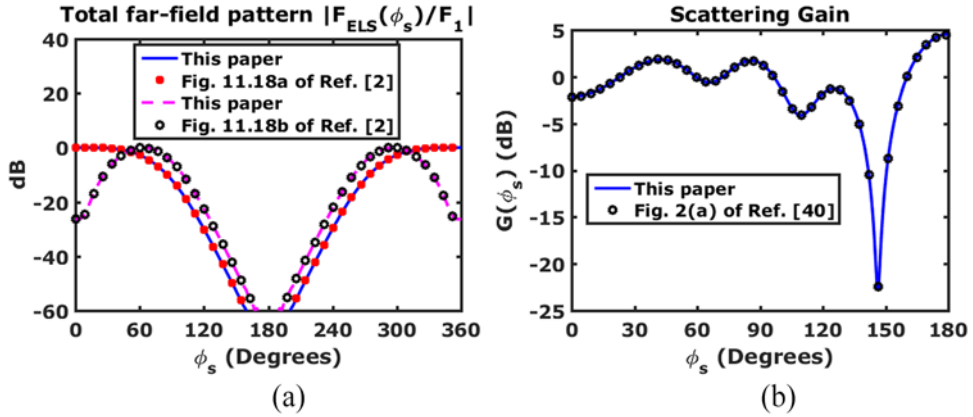


Figure 10. (a) The normalized total far-field pattern of a strip loaded dielectric cylinder due to an ELS illumination based on the proposed theory in the limit ϵ_r approaches to infinity and $\mu_r = 1$. In this case, a strip loaded dielectric cylinder equivalently becomes a PEC cylinder and its total far-field pattern is compared with the total far-field pattern as given by Balanis [2] and both total far-field patterns being compared are in good agreement. (b) The computed scattering gain [40] of a dielectric cylinder without strip and excited by an ELS based on the proposed theory. The computed scattering gain based on the proposed theory is in good agreement with the scattering gain as given by Aslam et al.

https://doi.org/10.1017/S175907872500025X Published online by Cambridge University Press

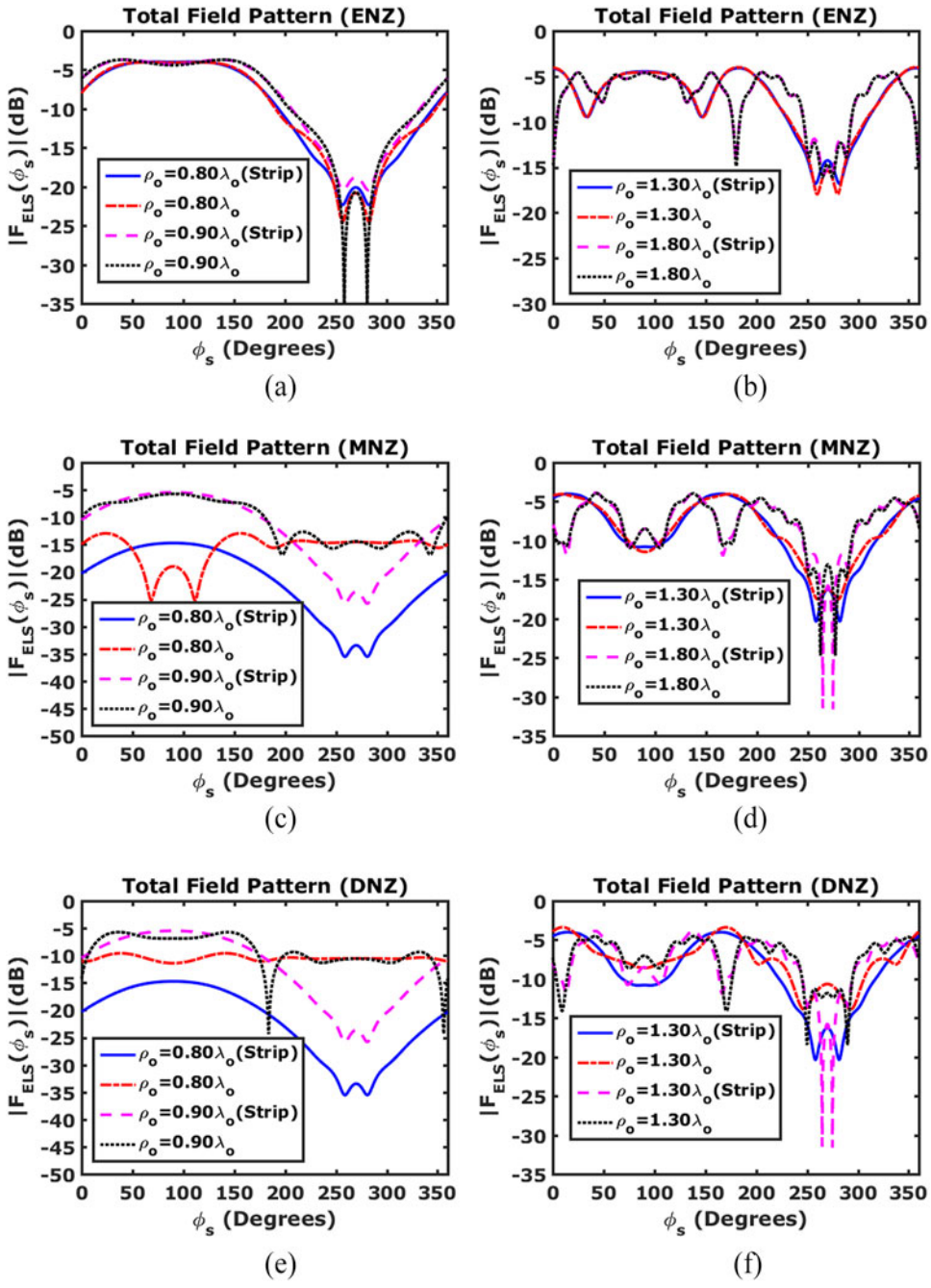


Figure 11. The influence of ELS locations upon the magnitudes of total field patterns for (a)–(b) ENZ cylinder and strip loaded ENZ cylinder, (c)–(d) MNZ cylinder and strip loaded MNZ cylinder, and (e)–(f) DNZ cylinder and strip loaded DNZ cylinder.

one can reduce the total field by 20 dB for this specific case. In the case of MLS excitation, it is seen from Fig. 12(a) that for a strip loaded ENZ cylinder with $\rho_o = 0.8\lambda_o$, there exists an enhancement of 15–20 dB in the magnitude of total field as compared to unloaded ENZ cylinder for ϕ_s lying between 65° and 110°. In the case of an unloaded MNZ cylinder with $\rho_o = 0.9\lambda_o$, the magnitude of total field is −62 dB at angles $\phi_s = 259°, 281°$ which is obvious from Fig. 12(c). For the same case, the magnitude of total field becomes almost −37 dB for a strip loaded MNZ cylinder at these considered angles, which signifies an enhancement of total field by 25 dB as compared to an unloaded MNZ cylinder. In the case of a DNZ cylinder, the total field for $\rho_o = 0.9\lambda_o$ becomes −50 dB at angles $\phi_s = 186°, 356°$ which is clear from Fig. 12(e). For this case, if a strip is inserted, then the total field becomes −30 dB at these specific angles. Thus, it is concluded that a strip can be used to enhance the total field by an amount of 20 dB at these specific angles.

Conclusions

The scattering characteristics of a strip loaded metamaterial cylindrical object under a plane and cylindrical wave excitation have

https://doi.org/10.1017/S175907872500025X Published online by Cambridge University Press

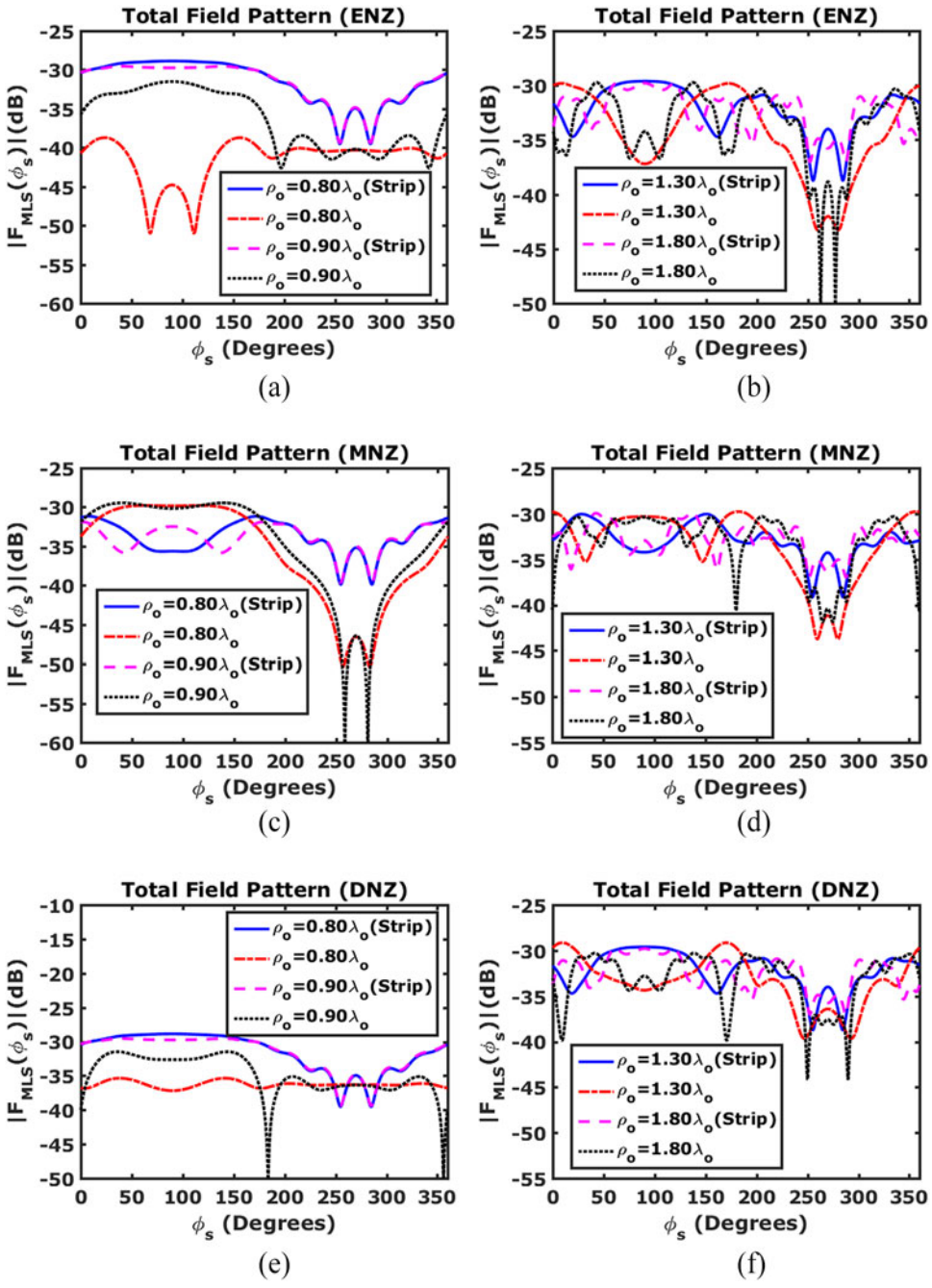


Figure 12. The magnitudes of total field patterns for (a)–(b) ENZ cylinder and strip loaded ENZ cylinder, (c)–(d) MNZ cylinder and strip loaded MNZ cylinder, and (e)–(f) DNZ cylinder and strip loaded DNZ cylinder for various locations of MLS.

been investigated. The types of metamaterial considered in the present study are SNZ and DNZ. The proposed problem has been solved using integral equations derived from Green's theorem along with the applications of usual tangential boundary conditions. In the case of plane wave excitation, the proposed numerical results are validated by comparing them with CST simulations. In this case, scattering characteristics of strip loaded dielectric and unloaded dielectric cylinder have also been shown and discussed for completeness. It is studied that by increasing the permittivity of a dielectric cylinder in the case of a strip loaded dielectric cylinder, the forward scattering increases whereas the backward scattering decreases. It is argued that there exists an enhancement of 3 dB in the back scattering for a strip loaded DNZ cylinder as compared to the back scattering of an unloaded DNZ cylinder for both types of incident polarization. For a specifically located ELS, there exists a significant reduction of 20 dB in the magnitude of total field from a strip loaded DNZ cylinder as compared to an unloaded DNZ cylinder at specific observation angles. In the case of a specific location of an MLS, a significant enhancement of 25 dB in the magnitude of total field from a strip loaded MNZ cylinder is noticed as compared to an unloaded MNZ cylinder in the specific observation directions. These above findings are interesting and find applications in the design of cylindrical metamaterial based devices.

https://doi.org/10.1017/S175907872500025X Published online by Cambridge University Press

Funding statement. This research received no specific grant from any funding agency, commercial or not-for-profit sectors.

Competing interests. The authors report no conflict of interest.

References

1. **Harrington RF** (1961) *Time-Harmonic Electromagnetic Fields*. New York: McGraw-Hill.
2. **Balanis CA** (2012) *Advanced Engineering Electromagnetics*, 2nd edn. Tempe, Arizona: John Wiley and Sons.
3. **Jin JM** (2015) *Theory and Computation of Electromagnetic Fields*. New Jersey: Wiley.
4. **Wait JR** (1955) Scattering of a plane wave from a circular dielectric cylinder at oblique incidence. *Canadian Journal of Physics* **33**(5), 189–195.
5. **Wang N** (1985) Electromagnetic scattering from a dielectric-coated circular cylinder. *IEEE Transactions on Antennas and Propagation* **33**(9), 960–963.
6. **Leviatan Y and Boag A** (1987) Analysis of electromagnetic scattering from dielectric cylinders using a multifilament current model. *IEEE Transactions on Antennas and Propagation* **35**(10), 1119–1127.
7. **Seker and SS and Schneider A** (1988) Electromagnetic scattering from a dielectric cylinder of finite length. *IEEE Transactions on Antennas and Propagation* **36**(2), 303–307.
8. **Henin BH, Elsherbeni AZ and Sharkawy MA** (2007) Oblique incidence plane wave scattering from an array of circular dielectric cylinders. *Progress in Electromagnetics Research* **68**, 261–279.
9. **Elsherbeni AZ and Hamid M** (1989) Scattering by a perfectly conducting strip loaded with a dielectric cylinder (TM case). *IEE Proceedings H-Microwaves, Antennas and Propagation* **136**(3), 185–190.
10. **Elsherbeni AZ and Jin L** (1992) Asymptotic scattering of electromagnetic waves from an array of dielectrically loaded conducting strips. *Journal of Electromagnetic Waves and Applications* **6**(1–4), 309–339.
11. **Tsalamengas JL, Vardiambasis IO and Fikioris GJ** (1995) Plane-wave scattering by strip-loaded circular dielectric cylinders in the case of oblique incidence and arbitrary polarization. *IEEE Transactions on Antennas and Propagation* **43**(10), 1099–1108.
12. **Tsalamengas LJ** (1996) Direct singular integral equation methods in scattering from strip-loaded dielectric cylinders. *Journal of Electromagnetic Waves and Applications* **10**(10), 1331–1358.
13. **Hamid AK and Hussein MI** (2003) Echo pattern width of a conducting strip loaded with a lossy dielectric layer. *International Journal of Applied Electromagnetics and Mechanics* **18**(4), 177–185.
14. **Engheta N and Ziolkowski RW** (2006) *Metamaterials: Physics and Engineering Explorations*. Hoboken, NJ: John Wiley and Sons.
15. **Engheta N, Alu A, Silveirinha MG, Salandrino A and Li J** (2006) DNG, SNG, ENZ and MNZ metamaterials and their potential applications. *MELECON 2006 - 2006 IEEE Mediterranean Electrotechnical Conference*. Malaga, Spain: pp. 258–261.
16. **Silveirinh MG and Engheta N** (2006) Tunneling of electromagnetic energy through subwavelength channels and bends using ε-near-zero materials. *Physical Review Letters* **97**(15), 157403.
17. **Edwards B, Alù A, Young ME, Silveirinha M and Engheta N** (2008) Experimental verification of epsilon-near-zero metamaterial coupling and energy squeezing using a microwave waveguide. *Physical Review Letters* **100**(3), 033903.
18. **Liu R, Cheng Q, Hand T, Mock JJ, Cui TJ, Cummer SA and Smith DR** (2008) Experimental demonstration of electromagnetic tunneling through an epsilon-near-zero metamaterial at microwave frequencies. *Physical Review Letters* **100**(2), 023903.
19. **Alu A, Silveirinh MG and Engheta N** (2007) Epsilon-near-zero metamaterials and electromagnetic sources: Tailoring the radiation phase pattern. *Physical Review B* **75**(15), 155410.
20. **Wang B and Huang KM** (2010) Shaping the radiation pattern with mu and epsilon-near-zero metamaterials. *Progress in Electromagnetics Research* **106**, 107–119.
21. **Adams DC, Inampudi S, Ribaudo T, Slocum D, Vangala S, Kuhta NA, Goodhue WD, Podolskiy VA and Wasserman D** (2011) Funneling light through a subwavelength aperture with epsilon-near-zero materials. *Physical Review Letters* **107**(13), 133901.
22. **Maas R, Parsons J, Engheta N and Polman A** (2013) Experimental realization of an epsilon-near-zero metamaterial at visible wavelengths. *Nature Photonics* **7**(11), 907–912.
23. **Gao J, Sun L, Deng H, Mathai CJ, Gangopadhyay S and Yang X** (2013) Experimental realization of epsilon-near-zero metamaterial slabs with metal-dielectric multilayers. *Applied Physics Letters* **103**(5), 051111.
24. **Pacheco-Pena V, Torres V, Beruete1 M, Cia MN and Engheta N** (2014) ϵ-near-zero (ENZ) graded index quasi-optical devices: Steering and splitting millimeter waves. *Journal of Optics* **16**(9), 094009.
25. **Pacheco-Pena V, Engheta N, Kuznetsov S, Gentselev A and Beruete M** (2017) Experimental realization of an epsilon-near-zero graded-index metalens at terahertz frequencies. *Physical Review Applied* **8**(3), 034036.
26. **Niu, Hu X, Chu S and Gong Q** (2018) Epsilon-near-zero photonics: A new platform for integrated devices. *Advanced Optical Materials* **6**(10), 1701292X.
27. **Guo Z, Jiang H, Zhu K, Sun Y, Li Y and Chen H** (2018) Focusing and super-resolution with partial cloaking based on linear-crossing metamaterials. *Physical Review Applied* **10**(6), 064048.
28. **Chen Y, Guo Z, Wang Y, Chen X, Jiang H and Chen H** (2020) Experimental demonstration of the magnetic field concentration effect in circuit-based magnetic near-zero index media. *Optics Express* **28**(11), 17064–17075.
29. **Huang X, Lai Y, Hang ZH, Zheng H and Chan CT** (2011) Dirac cones induced by accidental degeneracy in photonic crystals and zero-refractive-index materials. *Nature Materials* **10**(8), 582–586.
30. **Moitra P, Yang Y, Anderson Z, Kravchenko II., Briggs DP and Valentine J** (2013) Realization of an all-dielectric zero-index optical metamaterial. *Nature Photonics* **7**(10), 791–795.
31. **Liberal I and Engheta N** (2017) Near-zero refractive index photonics. *Nature Photonics* **11**(3), 149–158.
32. **Wang C, Qian C, Hu H, Shen L, Wang ZJ, Wang H, Xu Z, Zhang B, Chen H and Lin X** (2020) Superscattering of light in refractive-index near-zero environments. *Progress in Electromagnetics Research* **168**, 15–23.
33. **Awan ZA** (2014) Reflection and transmission properties of a wire grid embedded in a SNG or SZ medium. *Journal of Modern Optics* **61**(14), 1147–1151.
34. **Awan ZA** (2015) Effects of material parameters upon the dipolar scattering characteristics of uncoated or coated sphere. *Applied Optics* **54**(11), 3323–3330.
35. **Abbasi FR, Awan ZA and Hussain A** (2022) Backscattering cross-section from a metamaterial coated sphere covered with a metasurface. *International Journal of Microwave and Wireless Technologies* **14**(4), 445–455.
36. **McIsaac PR** (1979) A general reciprocity theorem. *IEEE Transactions on Microwave Theory and Techniques* **27**(4), 340–342.
37. **Awan ZA** (2017) Gain characteristics of a metamaterial coated slotted sphere. *Journal of Modern Optics* **64**(8), 807–818.
38. **Li C and Shen Z** (2003) Electromagnetic scattering by a conducting cylinder coated with metamaterials. *Progress in Electromagnetics Research, PIER* **42**, 91–105.
39. **Awan ZA and Seetharamdoo D** (2022) Enhancement of backscattering cross section from an equivalent human cylinder under oblique incidence. *IET Microwaves, Antennas & Propagation* **16**(8), 497–509.
40. **Aslam M, Saleem A and Awan ZA** (2017) Electric line source illumination of a chiral cylinder placed in another chiral background medium. *Journal of Modern Optics* **65**(8), 937–945.

https://doi.org/10.1017/S175907872500025X Published online by Cambridge University Press



Abdul Raqeeb received his Bachelor degree in Physics from Bahauddin Zakariya University, Multan, Pakistan in 2021. He has also received his Master of Philosophy degree in Electronics from the Quaid-i-Azam University, Islamabad, Pakistan in 2023. Currently, he is doing his Ph.D. at Wayne State University, Detroit, MI, USA. His main areas of research include electromagnetic scattering and metamaterials.



Zeeshan Akbar Awan received the Master of Philosophy form Department of Electronics, Quaid-i-Azam University, Islamabad, Pakistan in 2002. He has completed his Ph.D. degree in Electronics from the same university. He has worked as a Post-Doctoral candidate within LEOST Laboratory of the COSYS department in IFSTTAR, Lille, France from January to July 2018. He is presently an associate professor at the Department of Electronics, Quaid-i-Azam University, Islamabad, Pakistan. He has authored or co-authored more than 40 research articles. His research interests include electromagnetic scattering, metamaterials, metasurfaces, and antenna theory.



Arshad Hussain received the M.Phil form Department of Electronics, Quaid-i-Azam University, Islamabad, Pakistan in 2002. He completed his Ph.D. form State Key Laboratory of Analog and Mixed-Signal VLSI, Department of Electrical and Computer Engineering, Faculty of Science and Technology, University of Macau, Macau (SAR), China. He also completed 1-year Post-Doctorate from Department of Information and Communication Engineering, Chosun University, GwangJu, South Korea. He is currently working as Assistant Professor at the Department of Electronics, Quaid-i-Azam University, Islamabad, Pakistan. His current research interests are analog circuits, switched-capacitor circuits, design of low power high resolution delta-sigma ADCs, and electromagnetics.

https://doi.org/10.1017/S175907872500025X Published online by Cambridge University Press